

(XNC) ILLiad TN: 197253



**Journal of biological inorganic chemistry**  
**JBIC ; a publication of the Society of**  
**Biological Inorganic Chemistry.**

Vol: 13 Iss: 1 Month/Yr: January 2008 Pgs: 15-24

**Article Author:**

**Article Title:** Fadi Bou-Abdallah, N. Dennis Chasteen;  
Spin concentration measurements of high-spin (g $\approx$ 4.3)  
rhombic iron(III) ions in biological samples; the

**Patron:** Bou-Abdallah, Fadi

**Lending String:** \*XNC,ZGM,ZLM,UVV,XBM

ILL Number: 37795748



**Journal Title:** *Journal of biological inorganic chemistry JBIC ; a publication of the Society of Biological Inorganic Chemistry.*

**Location:** *electronic*

**ARIEL**

*Copy Charge: \$0.00*

*Billed via: IFM*

**Borrower Shipping Info:**

**Symbol:** *ZQM*

**Address:**

*IDS - LAND- SUNY POTSDAM  
POTSDAM*

**Fax:** *315-267-2744*

**Ariel:** *137.143.108.96*

**Odyssey:** *137.143.109.97*

**E-MailOK :**

# Spin concentration measurements of high-spin ( $g' = 4.3$ ) rhombic iron(III) ions in biological samples: theory and application

Fadi Bou-Abdallah · N. Dennis Chasteen

Received: 29 June 2007 / Accepted: 27 September 2007 / Published online: 12 October 2007  
© SBIC 2007

**Abstract** Electron paramagnetic resonance (EPR) signals at  $g' = 4.3$  are commonly encountered in biological samples owing to mononuclear high-spin ( $S = 5/2$ )  $\text{Fe}^{3+}$  ions in sites of low symmetry. The present study was undertaken to develop the experimental method and a suitable  $g' = 4.3$  intensity standard and for accurately quantifying the amount of  $\text{Fe}^{3+}$  responsible for such signals. By following the work of Aasa and Vänngård (*J. Magn. Reson.* 19:308–315, 1975), we present equations relating the EPR intensity of  $S = 5/2$  ions to the intensities of  $S = 1/2$  standards more commonly employed in EPR spectrometry. Of the chelates tested,  $\text{Fe}^{3+}$ –EDTA (1:3 ratio) in 1:3 glycerol/water (v/v), pH 2, was found to be an excellent standard for frozen-solution  $S = 5/2$  samples at 77 K. The spin concentrations of  $\text{Cu}^{2+}$ –EDTA and aqua  $\text{VO}^{2+}$ , both  $S = 1/2$  ions, and of  $\text{Fe}^{3+}$ –transferrin, an  $S = 5/2$  ion, were measured against this standard and found to agree within 2.2% of their known metal ion concentrations. Relative standard deviations of  $\pm 3.6$ ,  $\pm 5.3$  and  $\pm 2.9\%$  in spin concentration were obtained for the three samples, respectively. The spin concentration determined for  $\text{Fe}^{3+}$ –desferrioxamine of known  $\text{Fe}^{3+}$  concentration was anomalously low suggesting the presence of EPR-silent multimeric iron species in solution.

**Keywords** Spin concentrations · Iron electron paramagnetic resonance · Siderophores · Mononuclear iron · Non-heme iron proteins

## Abbreviations

DF Desferrioxamine  
EPR Electron paramagnetic resonance  
Mops 3-(*N*-Morpholino)propanesulfonic acid  
NTA Nitrilotriacetate  
Tris Tris(hydroxymethyl)aminomethane

## Introduction

Electron paramagnetic resonance (EPR) signals occurring at  $g' \sim 4.3$  from mononuclear high-spin  $\text{Fe}^{3+}$  ions in sites of low symmetry are commonly found in a variety of solid-state materials, chelates and metalloproteins [1–10]. Their origin was first described in 1960 by Castner et al. [3] in studies of glass matrices (Fig. 1). Historically,  $g' = 4.3$  signals encountered in protein preparations were usually attributed to “garbage” iron from nonspecifically bound  $\text{Fe}^{3+}$  or from  $\text{Fe}^{3+}$  in a denatured active site. During the early years of bioinorganic chemistry, only two bona fide non-heme iron proteins exhibiting such signals were known, namely, transferrin [5] and protocatechuate dioxygenase [6]. In the intervening years, other non-heme iron proteins with functional mononuclear Fe(II)/Fe(III) sites exhibiting  $g' = 4.3$  signals in one or more states were discovered and characterized. These include intradiol dioxygenases, pterin and  $\alpha$ -ketoglutarate dependent hydrolyases (reviewed in [1]), bacterial iron carrier proteins [7] and various siderophores [9, 10]. The siderophore

**Electronic supplementary material** The online version of this article (doi:10.1007/s00775-007-0304-0) contains supplementary material, which is available to authorized users.

F. Bou-Abdallah · N. D. Chasteen (✉)  
Department of Chemistry,  
University of New Hampshire,  
Durham, NH 03824, USA  
e-mail: ndc@cisunix.unh.edu

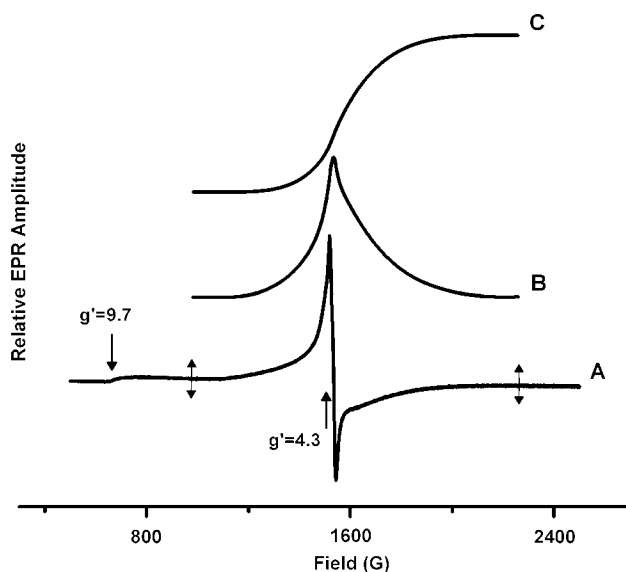


**Fig. 1** Electron paramagnetic resonance (EPR) spectrum of a borosilicate glass sample collected at 77 K. *A* First-derivative, *B* absorption and *C* integrated absorption curve. Limits of integration are indicated by double-headed arrows

desferrioxamine B (Desferyl<sup>®</sup>) has been widely used for treating diseases of iron overload and more recently the  $g' = 4.3$  signal of the  $\text{Fe}^{3+}$ –desferrioxamine (DF) complex has been employed to assess the “free iron pool” in the single-cell organisms *Escherichia coli* [11] and *Saccharomyces cerevisiae* [12, 13], in hepatocytes [14], in liver tissue homogenates [15] and in the whole worm *Caenorhabditis elegans* [16]. Mononuclear  $g' = 4.3$   $\text{Fe}^{3+}$  species have also been observed during the deposition of iron in mammalian and bacterial ferritins [17, 18] and during the delivery of iron from transferrin to its receptor [19]. The spectral details of the observed EPR signal as well as its intensity (as it relates to the amount of mononuclear  $\text{Fe}^{3+}$  present) are important for determining whether the observed iron is functional or simply adventitious.

Usually, the EPR spectra of  $S = 5/2$  spin systems can be adequately described by the spin Hamiltonian given by Eq. (1) [20, 21]. The first term represents the field-dependent Zeeman interaction:

$$H = g\beta \times (B_x S_x + B_y S_y + B_z S_z) + D(S_z^2 - 1/3 \times S^2) + E(S_x^2 - S_y^2), \quad (1)$$

where  $g$  is the electron  $g$  factor,  $\beta$  is the Bohr magneton,  $B_x$ ,  $B_y$  and  $B_z$  are the components of the applied magnetic field and  $S_x$ ,  $S_y$  and  $S_z$  are the spin angular momentum operators in the coordinate system of the spin. The second and third terms represent the zero-field interaction, where  $D$  and  $E$  are the zero-field splitting parameters arising from spin–orbit coupling of the ground state with excited states.

Occasionally higher-order cubic and quartic terms are needed to describe the spin system [2, 22]. Since the metal ion ground state derives from an atomic  $^6\text{S}$  state, the true  $g$  factor to a good approximation is isotropic with a value of 2.00. For high-spin  $\text{Fe}^{3+}$  in sites of low symmetry, the zero-field parameter is relatively small,  $|D| < 2 \text{ cm}^{-1}$  [1, 2, 20, 21], an important characteristic for spin quantification of these systems (vide infra).

The energy level diagram for an  $S = 5/2$  spin system of purely rhombic symmetry, i.e.,  $E/D = 1/3$ , in which  $h\nu < D$  is shown in Fig. 2 [22]. This is the situation most frequently encountered for non-heme iron. The three sets of Kramers doublets of the  $S = 5/2$  manifold of states are separated by  $3.53D$  in zero field (Fig. 2). In high magnetic field ( $D \ll g\beta B$ ), the six states correspond to pure  $M_s = \pm 1/2, \pm 3/2$  and  $\pm 5/2$  spin states and only transitions following the selection rule  $\Delta M_s = \pm 1$  are allowed. However, the six states become highly mixed in low field owing to the  $E(S_x^2 - S_y^2)$  term in the Hamiltonian. This mixing allows resonance absorptions to occur *within* each of the pair of states, i.e.,  $1 \leftrightarrow 2, 3 \leftrightarrow 4$  and  $5 \leftrightarrow 6$  of Fig. 2. The pair of states within each Kramers doublet can be treated as a fictitious spin  $S' = 1/2$  with an effective  $g'$  determined by the field position of the resonant absorption. The values of  $g'$  for the transitions within the upper and lower doublets ( $1 \leftrightarrow 2$  and  $5 \leftrightarrow 6$ ) are highly dependent on the orientation of the field and range from  $g' = 0.60$  to  $g' = 9.69$ . This large anisotropy in  $g'$  produces resonance fields between approximately 700 and approximately 11,000 G at X-band frequency (9.5 GHz). The weak feature at approximately 700 G ( $g' \sim 9.7$ ) commonly seen in the spectrum of  $\text{Fe}^{3+}$  (Fig. 1) has contributions from both the  $1 \leftrightarrow 2$  and the  $5 \leftrightarrow 6$  transitions and corresponds to low-field turning points in their resonance fields  $B_y$  and  $B_z$ , respectively (Fig. 2). Resonances in spectra of powder or frozen-solution samples from “turning points” within the  $xz$ ,  $yz$ , and  $xy$  principal planes also occur (not shown) [2, 20, 21]. In contrast, the transition within the middle pair of states  $3 \leftrightarrow 4$  is isotropic with  $g'$  predicted to be  $g' = 30/7 = 4.286$  [20, 22]. The isotropic character of this transition produces an EPR signal whose amplitude is deceptively strong relative to the amount of iron producing it and accounts for the fact that trace amounts of rhombic high-spin  $\text{Fe}^{3+}$  in most materials are readily observed in the EPR spectrum (Fig. 1).

Successful simulations of EPR spectra of rhombic or near-rhombic  $\text{Fe}^{3+}$  centers using eigenfield perturbation theory [2] or full matrix calculations in the extensive work of Yan and Gaffney [4], Gaffney and Silverstone [20] and Weisser et al. [23] have been reported. The theory of intensities of powder line shapes for quantitative EPR of various spin systems was originally presented by Aasa and Vännngård [24] in their classic paper. However, to our

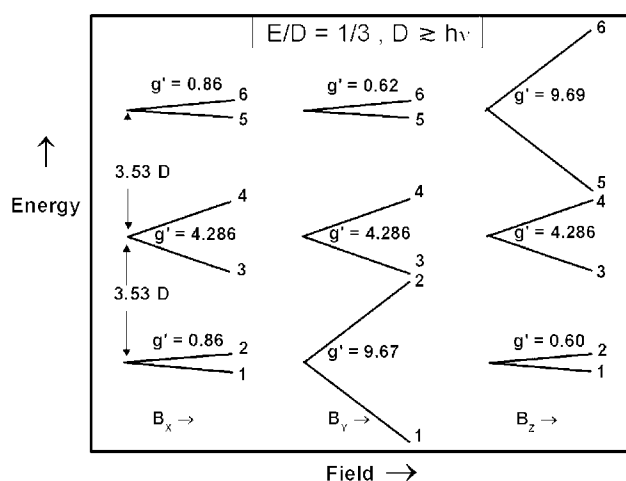


**Fig. 2** Energy diagram of the three Kramers doublets as a function of the magnetic field along the principal  $x$ ,  $y$  and  $z$  axes for a rhombic  $S = 5/2$  spin system [22]

knowledge, a detailed experimental analysis of the intensities of  $g' = 4.3$  signals for the purpose of accurate spin concentration determinations has not been carried out nor has a  $g' = 4.3$  intensity standard for quantitative EPR measurements of unknown  $g' = 4.3$  signals been proposed. In the present paper, we extend the work of Aasa and Vännegård [24] and examine the factors that must be considered when carrying out spin concentration measurements on  $g' \sim 4.3$  signals, relate the results to the more common measurement with  $S = 1/2$  ( $g \sim 2$ ) standards and develop a  $g' = 4.3$  standard for quantitative work. Application of this method to quantifying  $\text{Fe}^{3+}$  in transferrin and in ferrioxamine reveals that the  $g' = 4.3$  signal accounts for all of the iron in transferrin but only about 50% of the iron in ferrioxamine samples. Our findings should be of use in studies of iron binding proteins and chelators in biology as well as in studies of a variety of solid-state materials where  $g' \sim 4.3$  EPR signals from  $\text{Fe}^{3+}$  are common.

## Materials and methods

The  $\text{Fe}^{3+}$ -EDTA titration producing a 1:1 complex was conducted by adding microliter quantities of a 1,000 ppm (equivalent to 17.8 mM) Fe atomic absorption standard in dilute nitric or hydrochloric acid (Ricca Chemical Company, Arlington, TX, USA) to 0.40 mM EDTA in 1:3 v/v glycerol/water, pH  $\sim 5$ . The resulting  $\text{Fe}^{3+}$ -EDTA solution of pH 3–4 was then diluted in 3-(*N*-morpholino)propane-sulfonic acid (Mops) buffer to give a final concentration of 0.3 mM EDTA in 0.10 M buffer, pH 7.12 in 1:3 v/v glycerol. The EDTA solution was prepared by dissolving disodium EDTA dihydrate salt (Pierce, Rockford, IL, USA)

in 1:3 v/v glycerol/water. The  $\text{Fe}^{3+}$ -EDTA titration producing the 1:2 complex was done in the same way except that the standard  $\text{Fe}^{3+}$  solution was added directly to 0.4 mM EDTA in 0.16 M Mops buffer, pH 7.15, 1:3 v/v glycerol/water.

The 0.5 mM  $\text{Fe}^{3+}$ -EDTA solution ultimately used as a standard solution for quantitative EPR measurements was prepared by adding 14.4  $\mu\text{L}$  of 17.8 mM (1,000 ppm) standard  $\text{Fe}^{3+}$  in dilute hydrochloric acid (pH  $\sim 2$ ) to 500  $\mu\text{L}$  of 1.8 mM EDTA solution (pH  $\sim 2.0$ ) in 1:3 v/v glycerol/water, to give a final  $\text{Fe}^{3+}$  concentration of 0.498 mM and an  $\text{Fe}^{3+}$ -to-EDTA ratio of 1/3 at pH  $\sim 2$ . A more dilute 50  $\mu\text{M}$   $\text{Fe}^{3+}$ -EDTA standard sample, which is closer to the concentrations employed in *in vivo* work, gave the same EPR intensity (double integral) per iron as the more concentrated 0.5 mM standard.

The  $\text{Cu}^{2+}$ -EDTA solution for EPR analysis was prepared in a 1:3  $\text{Cu}^{2+}$ -to-EDTA ratio by adding 15.9  $\mu\text{L}$  of 1,000 ppm (equivalent to 15.73 mM) atomic absorption standard to 500  $\mu\text{L}$  of 0.1 M Mops buffer containing 1.5 mM EDTA in 1:3 glycerol/water, pH 7.0, to give a final concentration of 0.500 mM  $\text{Cu}^{2+}$  and a ratio of 1:3  $\text{Cu}^{2+}$  to EDTA.

The 0.504 mM  $\text{VO}^{2+}$  solution for EPR analysis was prepared by adding 3.6  $\mu\text{L}$  of 0.28 M stock solution of vanadyl sulfate trihydrate, pH 1.55 (Fisher Scientific, Morris Plains, NJ, USA) to 2.0 mL of dilute  $\text{H}_2\text{SO}_4$  (pH 1.5) in 1:3 glycerol/water prepared by mixing 3.75 mL of a dilute solution of  $\text{H}_2\text{SO}_4$ , pH  $\sim 1.5$  with 1.250 mL of glycerol. The final concentration of vanadium was determined by its absorbance,  $\epsilon_{750 \text{ nm}} = 18.0 \text{ M}^{-1} \text{ cm}^{-1}$  [25].

Monoferric human serum transferrin at 0.493 mM  $\text{Fe}^{3+}$  concentration for EPR analysis was prepared by adding 43.8  $\mu\text{L}$  of 7.42 mM  $\text{Fe}^{3+}$ -nitrilotriacetate (NTA) solution (1:2 ratio of Fe to NTA) to 500  $\mu\text{L}$  of 1.0 mM apotransferrin (Calbiochem, La Jolla, CA, USA) in 20 mM  $\text{NaHCO}_3$ , 50 mM Mops, pH 7.0. The concentration of bound  $\text{Fe}^{3+}$  was verified by its absorbance ( $\epsilon_{460 \text{ nm}} = 2,500 \text{ M}^{-1} \text{ cm}^{-1}$ ) [5]. The  $\text{Fe}^{3+}$ -NTA solution was freshly prepared by adding dropwise 125  $\mu\text{L}$  of 35.8 mM disodium nitrilotriacetate [prepared by dissolving nitrilotriacetic acid (Aldrich, Milwaukee, WI, USA) in water] to 125  $\mu\text{L}$  of 17.8 mM  $\text{Fe}^{3+}$  (1,000 ppm atomic absorption standard) with stirring. The pH was then adjusted to approximately 4.5 by the slow dropwise addition of 50  $\mu\text{L}$  of 0.7 M NaOH with stirring to give a final  $\text{Fe}^{3+}$ -NTA concentration of 7.42 mM.

Desferrioxamine B mesylate (Desferal<sup>®</sup>) was obtained from Sigma-Aldrich (St Louis, MO, USA) or from Novartis (Basel, Switzerland). The  $\text{Fe}^{3+}$ -DF solution was prepared similarly to  $\text{Fe}^{3+}$ -EDTA. Microliter quantities of an  $\text{FeCl}_3$  or  $\text{Fe}(\text{NO}_3)_3$  atomic absorption standard (1,000 ppm, equivalent to 17.8 mM) were added to a 0.25–1.5 mM DF

solution prepared in H<sub>2</sub>O and 1:3 glycerol/water (v/v) at pH 2, or in 0.05–0.1 M Mops or tris(hydroxymethyl)aminomethane (Tris)/HCl and 1:3 glycerol/water, pH 6.7–7.2, to give ratios of 1:1 or 1:3 Fe to DF. The concentration of the Fe<sup>3+</sup>–DF complex was independently determined from its absorbance ( $\epsilon_{420\text{ nm}} = 2,865\text{ cm}^{-1}\text{ M}^{-1}$ ) [13] (Fig. S1). Because of the reduced EPR intensity of these samples (i.e., approximately 50%) compared with those of Fe<sup>3+</sup>–EDTA, attempts to produce Fe<sup>3+</sup>–DF samples giving stronger EPR signals were made using FeSO<sub>4</sub> or Fe<sup>3+</sup>–NTA (1:2) also as the iron source. In both instances, the double integral of the EPR spectra remained only about half that of the spectrum of the Fe<sup>3+</sup>–EDTA standard sample under the same experimental conditions. To test the possibility that DF may have reduced Fe<sup>3+</sup> to Fe<sup>2+</sup>, 2  $\mu\text{L}$  of ferrozine (0.025 M) was added to a freshly prepared sample. No pink color of the (ferrozine)<sub>3</sub>–Fe<sup>2+</sup> complex developed, indicating the absence of Fe<sup>2+</sup> in the solution.

EPR measurements were carried out at 77 K in a liquid N<sub>2</sub> quartz Dewar insert using a Bruker ELEXSYS E560 spectrometer with a critically coupled high-sensitivity super-high-*Q* cavity. About 250  $\mu\text{L}$  of sample was introduced with a long-needled syringe into the bottom of a 3-mm inner diameter, 4-mm outer diameter quartz EPR tube (Wilmad 707-SQ-250M) to give a solution height of approximately 40 mm. The measured inner and outer dimensions of the EPR tubes had relative standard deviations of  $\pm 1.25\%$ . EPR amplitudes of spectra of the same sample in different tubes were within this deviation. Care was taken to accurately reposition the Dewar insert and sample tube in the cavity each time. The spectrometer and microwave bridge were allowed to warm up and stabilize for about 1 h prior to measurements. All spectra were gathered with a single scan under the same nonsaturating conditions: namely, power 0.271 mW; modulation amplitude 10 G; receiver gain +60 dB; scan time 67.77 s; time constant 163.84 ms; scan range 2,000 G and center field 1,500, 3,200 or 3,400 G for Fe<sup>3+</sup>–EDTA, Fe<sup>3+</sup>–human transferrin and Fe<sup>3+</sup>–DF, Cu<sup>2+</sup>–EDTA and VO<sup>2+</sup>, respectively; number of data points 8,192; and conversion time 20.48 ms. Although the scan rate employed is not optimum for resolving fine structure in the *S* = 1/2 spectra such as those of VO<sup>2+</sup>, it does not affect the value of the double integral and saves time when measuring a large number of samples as was the case in the present work. The spectrum of a sample containing either H<sub>2</sub>O or 0.05–0.1 M Mops buffer in 1:3 v/v glycerol/water served as a blank. The spectrum of the blank had a slightly nonlinear downward sloping baseline to high field owing to trace amounts of O<sub>2</sub> in the liquid N<sub>2</sub>. Before the spectra of the various samples were integrated using the Bruker Xepr software, the background spectrum was scaled and subtracted from all spectra to give the same EPR baseline value at

the beginning and end of the scan. Linear baseline corrections were subsequently employed for first and second integrations.

## Results and discussion

### An EPR intensity standard

In principle any *S* = 1/2 compound such as a VO<sup>2+</sup> or a Cu<sup>2+</sup> chelate can be used as an intensity standard for *S* = 5/2 (*g*' = 4.3) signals as illustrated below. However, in order to minimize sources of error, it is advantageous to use a standard that exhibits a *g*' = 4.3 EPR spectrum similar to that of the unknown. As a result, the number of intensity corrections is fewer and issues regarding the linearity of instrument settings are largely avoided. A suitable Fe<sup>3+</sup> standard for quantitative EPR measurements should be easy to prepare from a readily available ligand, exist in 100% monomeric form in aqueous solution and exhibit a sharp, well-defined *g*' = 4.3 signal at 77 K. Because of the propensity of Fe<sup>3+</sup> complexes to form EPR-silent  $\mu$ -oxo(hydroxo) bridged species in aqueous media [26, 27], the EPR spectra of Fe<sup>3+</sup> complexes with common ligands such as citrate, NTA and EDTA show quite variable intensity. For the various ligands tested, the EPR spectrum of Fe<sup>3+</sup> complexed with EDTA showed the strongest *g*' = 4.3 EPR signal (peak-to-trough width 23 G) and the largest value for the double integral (Fig. 3). We therefore sought to find solution conditions which optimized the strength of the EPR signal of this

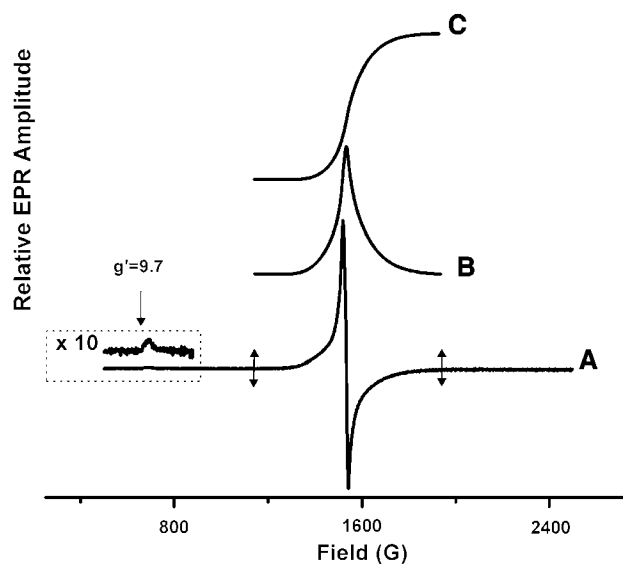


**Fig. 3** EPR spectrum of Fe<sup>3+</sup>–EDTA. **A** First-derivative, **B** absorption and **C** integrated absorption curve. Limits of integration are indicated by *double-headed arrows*. Conditions 0.498 mM Fe<sup>3+</sup>–EDTA, 1:3 ratio, pH 2.0 with HCl in 1:3 v/v glycerol/water, 77 K

complex and which would quantitatively account for all of the  $\text{Fe}^{3+}$  present in the sample.

Figure 4a shows the double integral of the  $g' = 4.3$  EPR signal for a series of samples of different  $\text{Fe}^{3+}$ -to-EDTA ratio prepared by adding ferric nitrate to an unbuffered disodium EDTA solution at pH 5 and then diluting this solution to pH 7 with stock Mops buffer to give a final solution concentration of 0.5 mM EDTA in 50 mM Mops, pH 7 (see “Materials and methods”). The titration demonstrates that a 1:1 complex is formed and that iron added beyond the equivalence point does not contribute to the EPR signal, owing to formation of EPR-silent dimeric and/or oligomeric species. Extrapolation of the early linear portion of the titration where EDTA is in excess to the 1:1 equivalence point (Fig. 4a, dashed line) indicates that the signal per unit concentration of  $\text{Fe}^{3+}$  has decreased by 12%, suggesting increased iron hydrolysis and  $(\text{Fe}^{3+}\text{-EDTA})_2$  dimer formation when EDTA is present in a 1:1 stoichiometric amount (Fig. 4a). Both monomeric and dimeric 1:1  $\text{Fe}^{3+}$  complexes with EDTA are well known, the metal ion being seven-coordinate in both instances [28, 29].

We also carried out a titration of  $\text{Fe}^{3+}$  directly into 0.5 mM EDTA in 160 mM Mops pH 7 (Fig. 4b). Under these conditions a complex with an apparent stoichiometry of 1:2  $\text{Fe}^{3+}$ -to-EDTA is formed. The double integral per  $\text{Fe}^{3+}$  added in the linear portion of the titration, i.e., for the first three data points, was 4% below that in Fig. 4a, indicating that sample preparation through direct  $\text{Fe}^{3+}$  addition at the higher pH of 7 compared with pH 5 produces slightly less EPR-observable mononuclear  $\text{Fe}^{3+}$  species.

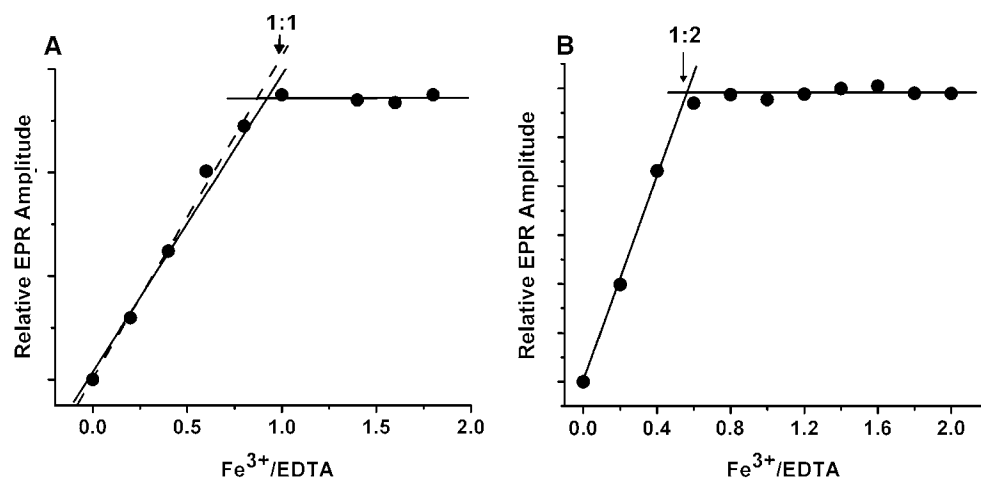


**Fig. 4** The EPR amplitude as a function of  $\text{Fe}^{3+}$ -to-EDTA ratio. **a** Each point on the graph represents a new sample, whereby microliter quantities of a 1,000 ppm  $\text{Fe}^{3+}$  standard solution (Ricca Chemical, in dilute  $\text{HNO}_3$ ) were added to 0.4 mM EDTA solution prepared in  $\text{H}_2\text{O}$ , pH  $\sim 5.0$  containing 1:3 v/v glycerol/water while stirring. The resulting Fe–EDTA solution was then diluted in

Taken together, the two titrations illustrated in Fig. 4 demonstrate that the method of sample preparation is important and that samples prepared with an excess of EDTA and at lower pH produce stronger EPR signals. Therefore, we prepared an  $\text{Fe}^{3+}$ –EDTA solution with a 1:3  $\text{Fe}^{3+}$ -to-EDTA ratio at pH 2, where iron hydrolysis would be minimal. The EPR spectrum of the complex was identical in line shape and width to that prepared at pH 7 for the 1:1 complex but was 3.5% more intense than the spectrum of the strongest pH 7 sample on a per  $\text{Fe}^{3+}$  basis in the titration illustrated in Fig. 4a. Accordingly, the 0.5 mM  $\text{Fe}^{3+}$ –EDTA sample prepared in acid solution was examined as a possible  $S = 5/2$  intensity standard. Its EPR intensity (double integral) was compared with those of other paramagnetic  $S = 5/2$  and  $S = 1/2$  standard samples at the same metal ion concentration.

#### Quantitative EPR of $S = 1/2$ and $S = 5/2$ spin systems

To make accurate quantitative measurements and comparisons between the various kinds of samples, several factors must be taken into account. For  $g' = 4.3$  signals, the range of integration must be kept as narrow as possible to avoid including significant contributions from the underlying resonances from transitions within the lower and upper Kramers doublets ( $1 \leftrightarrow 2$  and  $5 \leftrightarrow 6$ ) which span the entire spectrum (see “Introduction”). Working with a narrow range also minimizes the influence of the base line and base line correction on the value of the double integral. We typically plot the value of the double integral as a

3-(*N*-morpholino)propanesulfonic acid (Mops) buffer to give final concentrations of 0.1 M buffer, pH 7.12 and 25% v/v glycerol and 0.3 mM EDTA. **b** Samples were prepared similarly but this time by adding microliter quantities of the same  $\text{Fe}^{3+}$  standard solution to 0.4 mM EDTA in 0.16 M Mops buffer, pH 7.12 containing 1:3 v/v glycerol/water

function of the range of integration and average the values obtained on the plateau as shown in Fig. 5 for Fe<sup>3+</sup>–EDTA. If the  $g' = 9.7$  signal is included in the integration, the double integral will show a step increase. This increase can be particularly pronounced for spectra such as found for glass (Fig. 1) where the EPR amplitude gradually falls off to low field but does not return to zero until the field is below the  $g' \sim 9.7$  signal at approximately 700 G. (Step increases of 74% for glass, 85% for Fe<sup>3+</sup>–DF, 25% for Fe<sup>3+</sup>–human transferrin and 21% for Fe<sup>3+</sup>–EDTA were observed.) If the limits of integration are too large, the uncertainty in the double integral also increases markedly as illustrated in Fig. 5. We found no correlation between the peak-to-trough line width of the first-derivative  $g' = 4.3$  EPR signal and the optimal range of integration. We suggest that a plot such as in Fig. 5 always be done for both standards and unknowns and that an average of double integral values on the plateau be used in subsequent calculations.

For a given scan range, the normalized value of the double integral  $\bar{A}$  is given by Eq. 2:

$$\bar{A} = \frac{A}{\text{RG} \times \text{MA} \times \sqrt{P} \times \frac{1}{T} \times g_p^{\text{ave}} \times \text{CT}}, \quad (2)$$

where RG is the receiver gain, MA is the modulation amplitude in gauss,  $P$  is the microwave power in milliwatts,  $T$  is temperature in kelvin,  $g_p^{\text{ave}}$  is the average intensity factor over all orientations of the field (vide infra) and CT is the conversion time (the integration time per data point). Equation 2 assumes that the spectrum is not overmodulated

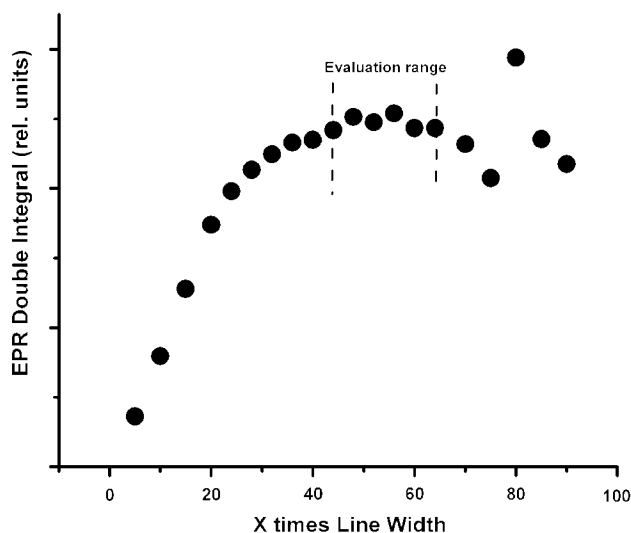


**Fig. 5** The double integral of the Fe<sup>3+</sup>–EDTA EPR spectrum (pH 2.0) of Fig. 3 as a function of the range of integration in terms of peak-to-trough line width. Line width 23 G

nor power-saturated and that the intensity follows the Curie law ( $1/T$  dependence). On Bruker spectrometers signal amplification is expressed in decibels, 6 dB corresponding to amplification by a factor of 2. Therefore, the receiver gain used for Eq. 2 is given by  $10^{\text{dB}/20}$ . If one chooses the “normalize spectrum” option in the Bruker Xepr software, the spectra are automatically scaled according to both the conversion time and the receiver gain, in which case Eq. 2 is reduced to Eq. 3:

$$\bar{A} = \frac{A'}{\text{MA} \times \sqrt{P} \times \frac{1}{T} \times g_p^{\text{ave}}}, \quad (3)$$

where  $A'$  is the double integral of the spectrum normalized for conversion time and receiver gain. In the present work, all measurements were done at 77 K, used the same modulation amplitude, power and receiver gain and employed the same number of data points and scan range. The EPR signal amplitude for the same sample at these settings over a period of 3 weeks varied less than 3% and more commonly less than 1%.

Aasa and Vänngård [24] give an approximate expression for the average intensity factor for field-swept powder spectra of a fictitious spin  $S' = 1/2$  based on the transition probability integrated over the magnetic field, namely,

$$g_p^{\text{ave}} \cong \frac{2}{3} \left[ (g_x^2 + g_y^2 + g_z^2) / 3 \right]^{1/2} + \frac{1}{3} [(g_x + g_y + g_z) / 3]. \quad (4)$$

This expression is accurate to within 1.5% for most applications [24]. More precise expressions for computing intensities are given by Gaffney and Silverstone [20]. For rhombic high-spin Fe<sup>3+</sup> the  $g$  factor is isotropic and predicted to be  $g_p^{\text{ave}} = 4.286$ . The actual value measured from the cross-over of the first-derivative spectrum in any case will be close to 4.3. For “axial” Cu<sup>2+</sup> and VO<sup>2+</sup> $S = 1/2$  complexes, the anisotropic  $g$  factors are readily obtained from the frozen-solution EPR spectrum where  $g_{\perp} = g_x = g_y$  and  $g_{\parallel} = g_z$ .  $g_p^{\text{ave}}$  is typically near 2.0 for these types of samples. In the work reported here, the values of  $g_p^{\text{ave}}$  in Table 1 were calculated from Eq. 4.

To relate the normalized double integral  $\bar{A}$  of the  $g' = 4.3$  Fe<sup>3+</sup>–EDTA standard to the spin concentrations of  $S = 5/2$  and  $S = 1/2$  samples, one must account for the thermal population of the middle Kramers doublet (Fig. 2). The fraction of spins  $f_{3,4}$  occupying this doublet in zero field is given by the following expression:

$$f_{3,4} = \frac{e^{-3.53D/kT}}{1 + e^{-3.53D/kT} + e^{-7.06D/kT}}, \quad (5)$$

where  $k$  is the Boltzmann constant expressed in  $\text{cm}^{-1} \text{K}^{-1}$ . Since  $|D| \leq 2 \text{ cm}^{-1}$  for all known  $g' = 4.3$  systems [1, 2,

**Table 1** Spin concentration results

Sample	$g_p^{avc}$ <sup>a</sup>	$\bar{A}$ <sup>b</sup>	Known concentration (mM)	Measured concentration (mM) <sup>c</sup>	Percent difference <sup>d</sup>
Fe <sup>3+</sup> –EDTA <sup>c</sup> (standard)	4.264 <sup>f</sup>	$1.67 \times 10^5$	0.498	–	–
Cu <sup>2+</sup> –EDTA <sup>g</sup>	2.218 <sup>h</sup>	$5.09 \times 10^5$	0.500	$0.506 \pm 0.018$	+1.2
VO <sup>2+</sup> <sup>i</sup>	1.943 <sup>j</sup>	$4.96 \times 10^5$	0.504	$0.493 \pm 0.026$	–2.2
Fe <sup>3+</sup> –Tf <sup>k</sup>	4.263 <sup>l</sup>	$1.64 \times 10^5$	0.493	$0.489 \pm 0.014$	–0.8
Fe <sup>3+</sup> –DF <sup>m</sup>	4.283 <sup>f</sup>	$0.86 \times 10^5$	0.498	$0.256 \pm 0.007$	–48.6

Tf human transferrin, DF desferrioxamine

<sup>a</sup> Intensity factor calculated from Eq. 4

<sup>b</sup> Normalized double integral calculated from Eq. 3

<sup>c</sup> Errors in reported spin concentrations represent propagated errors from standard deviations in the values of the double integrals of both the standard and unknowns

<sup>d</sup>  $100 \times (\text{measured concentration} - \text{known concentration})/\text{known concentration}$

<sup>e</sup> 1:3 Fe<sup>3+</sup> to EDTA in 1:3 glycerol/water, pH 2 with HCl. The concentration of Fe<sup>3+</sup> was obtained from dilution of an atomic absorption standard

<sup>f</sup> Value from the cross-over of the EPR signal

<sup>g</sup> 1:3 Cu<sup>2+</sup> to EDTA in 0.1 M 3-(*N*-morpholino)propanesulfonic acid (Mops), pH 7.0, 1:3 v/v glycerol/water. The concentration of Cu<sup>2+</sup> was obtained from dilution of an atomic absorption standard

<sup>h</sup> Calculated from Eq. 4 with  $g_x = g_y = 2.291$  and  $g_z = 2.068$  measured from the EPR spectrum

<sup>i</sup> VOSO<sub>4</sub> in 1:3 glycerol/water, pH 1.5 with H<sub>2</sub>SO<sub>4</sub>. The concentration of VO<sup>2+</sup> was obtained from its absorbance at 750 nm

<sup>j</sup> Calculated from Eq. 4 with  $g_x = g_y = 1.980$  and  $g_z = 1.932$  measured from the EPR spectrum

<sup>k</sup> In 20 mM NaHCO<sub>3</sub>, 50 mM Mops, pH 7.0, no glycerol. The concentration of Fe<sup>3+</sup> bound to Tf was determined from its absorbance at 460 nm

<sup>l</sup> Calculated from Eq. 4 with  $g_x = 4.404$ ,  $g_y = 4.267$  and  $g_z = 4.113$  measured from the EPR spectrum

<sup>m</sup> 1:3 Fe<sup>3+</sup> to DF in 0.1 M Mops, pH 7.12, 1:3 v/v glycerol/water. The concentration of Fe<sup>3+</sup> was obtained from dilution of an atomic absorption standard

20], the fractional population is calculated to be at least  $f_{3,4} = 0.331$  at 77 K, corresponding to one third of the spins. For Fe<sup>3+</sup>–EDTA solution,  $D = 0.70 \text{ cm}^{-1}$  ( $E/D = 0.328$ ) [30] and for Fe<sup>3+</sup> doped in a Co<sup>3+</sup>–EDTA lattice,  $D = 0.83 \text{ cm}^{-1}$  ( $E/D = 0.31$ ) [21]. Curie behavior must be demonstrated if measurements are made on a sample at a significantly lower temperature (e.g., 4.2–20 K) whose value of  $D$  is unknown. Otherwise the measured EPR signal intensity near liquid helium temperature may underestimate the amount of Fe<sup>3+</sup> present. It is safer, easier and more accurate to make measurements at 77 K where good temperature control is attained and the Kramers doublet states are equally populated. From the above analysis, it is evident that the measured double integral of the  $g' = 4.3$  signal at 77 K must be multiplied by 3 to account for the fact that only one third of the spins in the sample contribute to the observed signal.

The factor of 3 is unimportant when both the standard ( $\text{Std}_{S=5/2}$ ) and unknown ( $\text{X}_{S=5/2}$ ) samples are  $S = 5/2$  ions. In this instance, the relationship between the concentrations of standard and unknown is given by Eq. 6. The relationship between an  $S = 5/2$  standard and an  $S = 1/2$  unknown

( $\text{X}_{S=1/2}$ ) or a standard such as Cu<sup>2+</sup> and VO<sup>2+</sup> requires the factor of 3 as shown in Eq. 7.

$$[\text{X}_{S=5/2}] = [\text{Std}_{S=5/2}] \times \frac{\bar{A}_{\text{X},S=5/2}}{\bar{A}_{\text{Std},S=5/2}} \quad (6)$$

$$[\text{X}_{S=1/2}] = [\text{Std}_{S=5/2}] \times \frac{\bar{A}_{\text{X},S=1/2}}{3 \times \bar{A}_{\text{Std},S=5/2}} \quad (7)$$

Comparisons between samples of known spin concentration

To test the validity of these equations and the suitability of Fe<sup>3+</sup>–EDTA as an intensity standard, we measured the EPR spectra of the commonly used standards Cu<sup>2+</sup>–EDTA and aqua VO<sup>2+</sup> ion and of Fe<sup>3+</sup>–transferrin ( $D = 0.25 \text{ cm}^{-1}$ ,  $E/D = 0.30$  [31]) and ferrioxamine B ( $D = 0.5 \text{ cm}^{-1}$  [32]) and compared their known metal ion concentrations with those measured against the proposed Fe<sup>3+</sup>–EDTA standard. The first-derivative spectra and corresponding first and second integrals of the four samples are shown in Figs. 6,



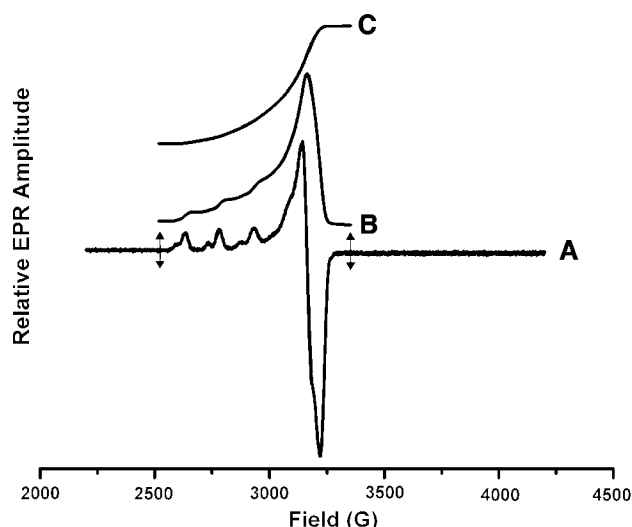


**Fig. 6** EPR spectrum of  $\text{Cu}^{2+}$ -EDTA. *A* First-derivative, *B* absorption and *C* integrated absorption curve. Limits of integration are indicated by *double-headed arrows*. Conditions 0.500 mM complex, 1:3  $\text{Cu}^{2+}$ -to-EDTA ratio in 0.1 M Mops, pH 7, 1:3 glycerol/water (v/v), 77 K. The minor  $\text{Cu}^{2+}$ -EDTA species represents approximately 25% of the total  $\text{Cu}^{2+}$  present

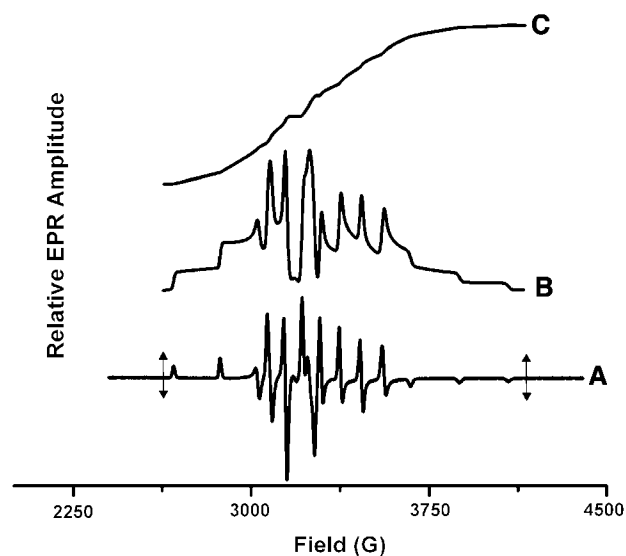


**Fig. 7** EPR spectrum of  $\text{VO}^{2+}$ . *A* First-derivative, *B* absorption and *C* integrated absorption curve. Limits of integration are indicated by *double-headed arrows*. Conditions 0.504 mM  $\text{VO}^{2+}$  in 1:3 glycerol/water (v/v), pH 1.5 with  $\text{H}_2\text{SO}_4$ , 77 K

7, 8 and 9. The integrations for all four samples are well behaved.

The calculated concentrations of the  $S = 1/2$   $\text{Cu}^{2+}$  and  $\text{VO}^{2+}$  ions and of  $S = 5/2$   $\text{Fe}^{3+}$  ion in transferrin based on the  $\text{Fe}^{3+}$ -EDTA standard agree within 2.2% of their known concentrations (Table 1). The relative standard deviations of their determined concentrations are  $\pm 3.6$ ,  $\pm 5.3$  and

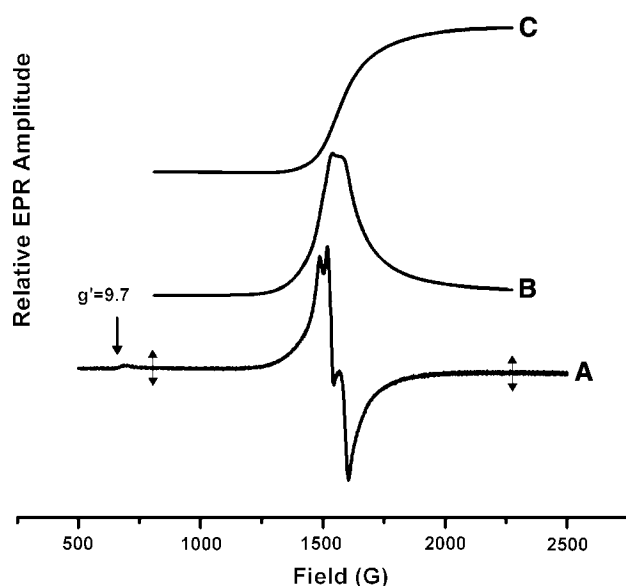


**Fig. 8** EPR spectrum of  $\text{Fe}^{3+}$ -human transferrin, pH 7.0. *A* First-derivative, *B* absorption and *C* integrated absorption curve. Limits of integration are indicated by *double-headed arrows*. Conditions 0.493 mM monoferric human transferrin in 20 mM  $\text{NaHCO}_3$ , 50 mM Mops, pH 7.0, 77 K

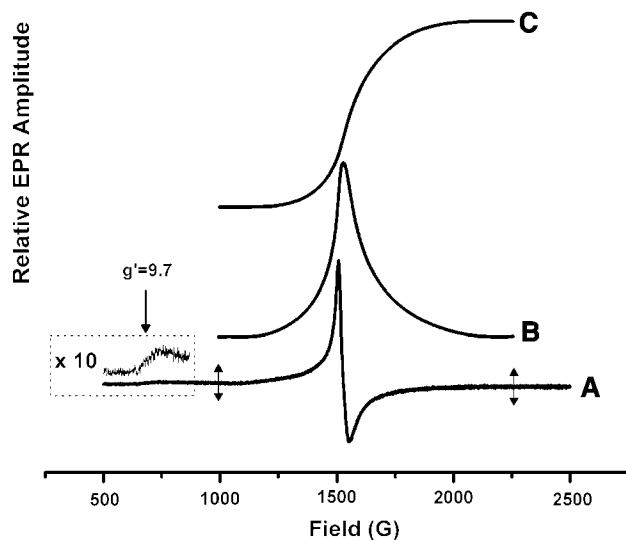


**Fig. 9** EPR spectrum of  $\text{Fe}^{3+}$ -desferrioxamine, pH 7.0. *A* First-derivative, *B* absorption and *C* integrated absorption curve. Limits of integration are indicated by *double-headed arrows*. Conditions 0.498 mM complex,  $\text{Fe}^{3+}$ -to-desferrioxamine ratio 1:3, 0.1 M Mops, pH 7.12, 1:3 v/v glycerol/water, 77 K

$\pm 2.9\%$ , respectively, and are within the 3–5% deviation expected if appropriate care is exercised in quantitative EPR measurements [33].  $\text{VO}^{2+}$  shows the largest relative standard deviation ( $\pm 5.3\%$ ) because the integration extends over a larger field range to capture the weak signals of the parallel lines in the wings of the spectrum (Fig. 7). The close correspondence between the  $\text{Fe}^{3+}$ -EDTA standard and  $\text{Fe}^{3+}$ -

transferrin is reassuring since transferrin has been previously used as a standard to quantify the amount of  $g' = 4.3$  iron in human lipoxxygenase [34]. Samples prepared in aqueous buffer or 1:3 v/v glycerol/water buffer gave double integrals that were the same within the errors stated above. However the spectra obtained with glycerol solutions had narrower line widths and had the advantage of no tube breakage from expansion of the solution upon freezing.

In contrast to the other samples, the  $g' = 4.3$  signal (46-G peak-to-trough width) for  $\text{Fe}^{3+}$ -DF underestimated the total amount of  $\text{Fe}^{3+}$  present by a factor of 2 (Table 1). The signal intensity exhibited Curie behavior near 77 K (data not shown) as expected for its small  $D = 0.5 \text{ cm}^{-1}$  [32]. We therefore explored the possibility that some of the iron added to the DF solution formed EPR-silent aggregates (dimers or oligomers) as well as monomers. Samples were prepared using various iron sources (i.e., ferrous sulfate followed by oxidation, ferric nitrate, ferric chloride or ferric nitrilotriacetate) but all gave the same spectrum of lower than expected integrated intensity. Similarly, spectra measured at pH 2 in water or pH 7 employing Mops or Tris buffer or in the presence or absence of glycerol had the same integrated intensity. A spectrophotometric titration of DF with  $\text{Fe}^{3+}$  while monitoring the 420 nm absorption band of the complex (Fig. S1) showed a 1:1 binding stoichiometry (Fig. S2). Similarly, an EPR spectrometric titration demonstrated that a 1:1 complex is responsible for the  $g' = 4.3$  signal (Fig. S3). The EPR intensity was also measured as a function of the concentration of  $\text{Fe}^{3+}$ -DF to look for evidence of a rapid dimer/monomer dissociative equilibrium but a simple linear dependence was found (Fig. S4). The lack of reduction of  $\text{Fe}^{3+}$  to  $\text{Fe}^{2+}$  species that would be EPR-silent under these conditions was demonstrated using ferrozine (see “Materials and methods”).

The reason for the low value of the double integral for  $\text{Fe}^{3+}$ -DF is unclear; however, it is known that the solution chemistry of  $\text{Fe}^{3+}$  and desferrioxamine B involves multiple species including dimers [35–38] and the ligand itself has 16 isomers, only two of which have been crystallized (as monomeric  $\text{Fe}^{3+}$  complexes) [39]. While  $D$  and  $E$  strain might be sources of the low value of the observed intensity [4, 23], the fact that the value of the double integral levels off with increasing limits of integration (Fig. 9) argues against this interpretation. Sergent et al. [14] in their study of the low molecular weight iron pool in hepatocytes also reported a significantly lower integrated EPR intensity with standard solutions of  $\text{Fe}^{3+}$ -DF than with standard solutions of  $\text{Fe}^{3+}$ -deferriprone, a finding in accord with the results observed here. Because of its low EPR intensity, its ability to remove  $\text{Fe}^{3+}$  from ferritin in cells and its weaker affinity for  $\text{Fe}^{3+}$  than deferriprone, Sergent et al. suggest that deferriprone is better suited for measuring low molecular weight iron in cells than is DF. On the basis of our findings

and those of Sergent et al. [14], it would be prudent to exercise caution when using DF to quantify the “free iron” in cells until the chemistry of this system and the origin of its low EPR signal are better understood. Furthermore, whether some components of the cell matrix might influence the EPR intensity is unknown.

## Conclusions

A reliable EPR standard (1:3  $\text{Fe}^{3+}$  to EDTA in pH  $\sim 2$  solution) devoid of hydrolysis problems has been developed for measuring  $\text{Fe}^{3+}$  concentrations associated with  $g' = 4.3$  EPR signals. Excellent agreement is obtained when comparisons are made with other  $S = 1/2$  and  $S = 5/2$  standards provided the proper equations are used. If appropriate care is exercised when measuring the spectrum and it is analyzed according to the guidelines presented here, relative standard deviations in spin concentration of less than 5% can be attained.

**Acknowledgement** This work was supported by grant R01 GM20194 from the National Institute of General Medical Sciences (to N.D.C.).

## References

1. Soloman EI, Grunold TC, Davis MI, Kemsley JN, Lee S-K, Lehnert N, Neese F, Skulan AJ, Yang Y-S, Zhou J (2000) *Chem Rev* 100:235–349
2. Scullane MI, White LK, Chasteen ND (1982) *J Magn Reson* 47:383–397
3. Castner T Jr, Newell GS, Holton WC, Slichter CP (1960) *J Chem Phys* 32:668–673
4. Yan A-S, Gaffney BJ (1987) *Biophys J* 51:55–67
5. Aasa R, Malmström BG, Saltman P, Vängård T (1963) *Biochim Biophys Acta* 75:203–222
6. Fujisawa H, Uyeda M, Kojima Y, Nozaki M, Hayaishi O (1972) *J Biol Chem* 247:4414–4421
7. Taboy CH, Vaughan KG, Mietzner TA, Aisen P, Crumbliss AL (2001) *J Biol Chem* 276:2719–2724
8. Citadini APS, Pinto APA, Araujo APU, Nascimento OR Costa-Filho AJ (2005) *Biophys J* 88:3502–3508
9. Ecker DJ, Lancaster JR Jr, Emery T (1982) *J Biol Chem* 257:8623–8626
10. Barclay SJ, Huynh BH, Raymond KN (1984) *Inorg Chem* 23:2011–2018
11. Keyer K, Imlay JA (1996) *Proc Natl Acad Sci USA* 93:13635–13640
12. Srinivasan C, Liba A, Imlay JA, Valentine JS, Gralla EB (2000) *J Biol Chem* 275:29187–29192
13. Srinivasan C, Gralla EB (2002) *Methods Enzymol* 349:173–180
14. Sergent O, Anger J-P, Lescoat G, Pasdeloup N, Cillard P, Cillard J (1997) *Cell Mol Biol* 43:783–800
15. Yegorov DY, Kozlov AV, Azizova OA, Validmirov YA (1993) *Free Radic Biol Med* 15:565–574
16. Pate KT, Rangel NA, Fraser F, Clement MHS, Srinivasan C (2006) *Anal Biochem* 358:199–207
17. Sun S, Chasteen ND (1994) *Biochemistry* 33:15095–15102

18. Yang X, Le Brun NE, Tompson AJ, Moore GR, Chasteen ND (2000) *Biochemistry* 39:4915–4923
19. Giannetti AM, Halbrooks PJ, Mason AB, Vogt TM, Enns CA, Bjorkman PJ (2005) *Structure* 13:1613–1623
20. Gaffney BJ, Silverstone HJ (1993) In: Berliner LJ, Reuben J (eds) *EMR of paramagnetic molecules*, vol 13. Plenum, New York, pp 1–57 and references therein
21. Aasa R (1970) *J Chem Phys* 52:3919–3930
22. Oosterhuis WT (1974) In: Dunitz JD, Hemmerich p, Holm RH, Ibers JA, Jørgensen CK, Williams RJP (eds) *Structure and bonding*, vol 20. Springer, New York, pp 59–99
23. Weisser JT, Nilges MJ, Sever MJ, Wilker JJ (2006) *Inorg Chem* 45:7736–7747
24. Aasa R, Vänngård T (1975) *J Magn Reson* 19:308–315
25. Fitzgerald JJ, Chasteen ND (1974) *Anal Biochem* 60:170–180
26. Schneider W (1988) *Chimia* 42:9–20
27. Kurtz DM Jr (1990) *Chem Rev* 90:585–606
28. Ozarowski A, McGarvey BR, Drake JR (1995) *Inorg Chem* 34:5558–5566
29. Mitzuta T, Wang J, Miyoshi K (1963) *Bull Chem Soc Jpn* 66:2547–2551
30. Lang G, Aasa R, Garbett K, Williams RJP (1971) *J Chem Phys* 55:4539–4548
31. Kretchmar SA, Teixeira M, Huynh BH, Raymond KN (1988) *Biol Met* 1:26–32
32. Bock JL, Lang G (1972) *Biochim Biophys Acta* 264:245–250
33. Mazur M (2006) *Anal Chim Acta* 561:1–15
34. Chasteen N, Grady JK, Skorey KI, Neden KJ, Riendeau D, Percival DM (1993) *Biochemistry* 32:9763–9771
35. Kiss T, Farkas E (1998) *J Incl Phenom Mol Recognit Chem* 32:385–403
36. Biruš M, Bradić Z, Krznarić G, Kujundžić N, Pribanić M, Wilkins PC, Wilkins RG (1987) *Inorg Chem* 26:1000–1005
37. Biruš M, Bradić Z, Krznarić G, Kujundžić N, Pribanić M (1983) *Inorg Chim Acta* 78:87–92
38. Valéria A, Simionato C, Cantú MD, Carrilho E (2006) *Microchem J* 82:214–219
39. Dhungana S, White PS, Crumbliss A (2001) *J Biol Inorg Chem* 6:810–818